Procedure for quasilocal measurements of electric fields in a plasma by using satellites of helium forbidden lines

M. P. Brizhinev, V. P. Gavrilenko, S. V. Egorov, B. G. Eremin, A. V. Kostrov, E. A. Oks, and Yu. M. Shagiev

Applied Physics Institute, USSR Academy of Sciences

(Submitted 19 November 1982)
Zh. Eksp. Teor. Fiz. **85**, 893–908 (September 1983)

An adiabatic theory of satellites of forbidden lines of helium and of helium-like ions is developed. The analytic results are valid not only for weak fields but also for strong ones, for which the hitherto existing solutions (obtained by Dirac's perturbation theory) are not valid. The theory developed serves as a basis for proposing a new principle of measuring the amplitude E_0 of oscillating electric fields (OEF) in a plasma. The principle is based on comparing the experimental ratio of the satellite intensities with the theoretical dependence of S_-/S_+ on E_0. This principle permits in essence to measure E_0 locally in a strong-field region even under conditions when this region is considerably smaller than the volume of the radiating plasma, without resorting to complicated experimental methods such as resonant fluorescence. Adiabatic theory of satellites has also made it possible to extend the technique of polarization analysis of OEF to include the case of strong fields. The theory developed can also be used for the diagnostics of OEF by means of the spectra of multiply charged ions. The indicated diagnostic procedures were tested in experiments in which a powerful microwave interacted with an inhomogeneous plasma. Reduction of the spectra near He I 4922 Å and He I 4471 Å, which are observed in both unpolarized and polarized light, lead to the following physical conclusions: 1) Amplification of the OEF, $E_{0p} > E_{0r}$, takes place in a pump field $E_{0r} > 0.5$ kV/cm near the critical-density surface; 2) the gain $K = E_{0p}/E_{0r}$ is a maximum at $E_{0r} \sim 2$ kV/cm; 3) the gain "saturates" with further increase of E_{0r} ($E_{0p} \gtrsim 7$ kV/cm at any E_{0r}); 4) what is predominantly amplified is the component $\mathbf{E}_{0p}$ parallel to the pump wave vector **k**. It can be concluded from the aggregate of the results that parametric instability develops in the plasma-resonance region and that intense Langmuir oscillations with energy density $W \lesssim 10^{-1} NT_e$ are excited.

PACS numbers: 52.70.Ds

§1. INTRODUCTION

Oscillating electric fields (OEF) play a decisive role in many physical processes in a plasma. The term OEF refers to the combination of the fields of the "intrinsic" plasma oscillations (plasma turbulence) and the fields that penetrate from the outside. The presence of OEF in a plasma is a feature of a host of experiments, including, e.g., the action of a powerful laser or microwave radiation and of electron or ion beam, reconnection of magnetic fields, shock-wave excitation, and passage of strong currents. The development of diagnostic methods for OEF in a plasma is therefore quite vital for many applied scientific and technical programs. Research is particularly intensive on spectroscopic methods of OEF diagnostics, one among the leading being the method of satellites of forbidden lines of helium (and of helium-like ions).

The satellite method was proposed by Baranger and Moser[1] in 1961 and was since repeatedly used. A description of experiments by this method, up to 1978, is contained in the reviews by Bekefi and Deutsch[2] and by Volkov *et al.*,[3] as well as in the book by Kuznetsov and Shcheglov.[4] From among the later experiments, mention can be made of Refs. 5 and 6. We emphasize that the theoretical treatment in Ref. 1 was restricted to the following assumptions: 1) absence of resonance relations of the type $(2j-1)\omega \approx \Delta$, where ω is the OEF frequency, $\Delta \equiv |\omega_{21}^{(0)}|$ is the spacing between the close levels of the atom, and $j = 1,2,3,...$; 2) $d_{12}E_0 \ll \Delta$, where d_{12} is the matrix element of the dipole moment and E_0 is the characteristic OEF intensity; 3) the OEF have an isotropic distribution in direction. Attempts to lift these restrictions were made in recent years.

The first restriction was lifted in Refs. 7 and 8, where single-quantum resonance $|\omega - \Delta| \ll \omega$ was considered. This was followed[9] by an analysis of the case of multiquantum resonance $|(2j-1)\omega - \Delta| \ll \omega$ ($j = 1,2,3,...$) in spectra of helium-like ions in a plasma produced by a laser or by a relativistic electron beam. In particular, a principally new effect was predicted, namely, the appearance, near the frequencies $\omega_{\rm res}^{(j)} = \omega_{10}^{(0)} + \Delta/(2j-1)$, of resonant satellites $S_{\rm res}^{(j)}$ in the space-integrated spectrum.

Attempts to lift the second restriction ($d_{12}E_0 \ll \Delta$) were initiated in Ref. 10, where the Dirac perturbation theory (DPT) yielded two more terms of the expansion in the parameter $d_{12}E_0/\Delta \ll 1$. This, however, did not lead to a substantial advance into the region of high OEF intensities. Computer calculations for stronger fields were performed in Ref. 11 for the lines He I 4922 Å and He I 4388 Å, using the theoretical approach of Autler and Townes.[12] In Ref. 11, however, the number of profiles calculated was rather limited. Furthermore, the inaccurate value $\Delta = 5.63$ cm^{-1} was

 0038-5646/83/090517-10$04.00

used for the He I 4922 Å line ($\Delta = 5.43$ cm^{-1} according to Martin's more accurate data[13]), making some of the results of Ref. 11 useless.

We note that most numerical calculations of Ref. 11 are devoted to the case of low frequencies $\omega \ll \Delta$. Yet it is precisely in this case that the problem can be solved analytically by adiabatic perturbation theory (APT). This solution is one of the main topics of the present paper. The results turn out to be valid also for strong fields, for which the APT cannot be used.

Finally, the third restriction (the assumption that the OEF are isotropic) was first lifted by Cooper and Ringler.[14] They considered the case of linear polarization of the OEF and analyzed the associated effects of anisotropy and polarization of the satellite emission. As indicated by them, their analysis is restricted to the framework of the DPT ($d_{12}E_0 \ll \Delta$). In the present work we have succeeded, using APT, in extending the procedure of the polarization analysis of OEF into the strong-field region. We note that in this region, as it turned out, the maximum degree of satellite polarization decreases.

To this day, in all experiments in which the satellite method was used, the OEF intensity E_0 was determined by comparing the experimentally measured ratio $S_\pm / I_A$ with the theoretical dependence of $S_\pm / I_A$ on E_0 (I_A is the intensity of the allowed line, S_- is the intensity of the nearby satellite, and S_+ the intensity of the far one). In a number of cases, however, the volume v_E in which the OEF exists and from which the satellites are emitted can be much less than the volume V from which the allowed spectral line is radiated. Such a situation (the presence of a form factor) is typical, e.g., of experiments in which plasma resonance is produced when a powerful electromagnetic wave interacts with an inhomogeneous plasma. The use of the dependence of $S_\pm / I_A$ on E_0 calls in this case for local measurements (with good spatial resolution) of the spectrum, using complicated experimental procedures (e.g., resonant fluorescence[1]). Yet in the case of strong fields it is possible, without using complicated experimental procedures that ensure spatial resolution, to determine the local intensity E_0 of the OEF. Such a quasi-local diagnostic method can be based on measurement of the ratio S_-/S_+ and comparison of the theoretical dependence of S_-/S_+ on E_0. This dependence is obtained in the present paper with the aid of APT, in which, as noted above, it is possible to advance into the strong-field region.

The theoretical results listed above are derived in §2 of the present paper. In §3 is described the experimental setup with which the interaction of a powerful microwave with a plasma was investigated, and the results of observations of satellites of forbidden lines of helium in unpolarized lines are reported. In these experiments we realized in practice a quasi-local OEF diagnostics method, based on measurement of the ratio S_-/S_+, and used the new theoretical results indicated above. In §4 are given the polarization-measurement results based the theoretical calculations of §2, including the strong-field region. In the experiments described in §§3 and 4 we succeeded in observing an increase of the field E_{0p} in the plasma compared with the pump field E_{0r} and in determining a number of regularities in the dependences of the magnitude and direction of the field $\mathbf{E}_{0p}$ on the value of E_{0r}. The discussion of these physical regularities as well as the prospects of further applications of the new theoretical results are the subject of §5.

§2. ADIABATIC THEORY OF SATELLITES OF FORBIDDEN LINES

1. We consider a system of three atomic levels 0, 1, 2 in which transition 2→0 corresponds to an allowed spectral line, and 1→0 to a (parity) forbidden line; the close levels 1 and 2 are coupled by a dipole transition. In the absence of an external field, the levels 0, 1, and 2 are characterized by wave functions (WF) $\psi_0 = \psi_{n'l'm'}$, $\psi_1 = \psi_{nlm}$, $\psi_2 = \psi_{nl''m'}$ and energies $\omega_0^{(0)}$, $\omega_1^{(0)}$, $\omega_2^{(0)}$ (we use in this section the atomic units $\hbar = m = e = 1$). In a linearly polarized electric field $\mathbf{E}(t) = \mathbf{E}_0 \cos \omega t$ the Schrödinger equation can be represented in the form

$$i\partial\psi/\partial t=(H_a+zE_0 \cos \omega t)\psi, \tag{1}$$

where H_a is the Hamiltonian of the isolated atom. Solution with the aid of the OPT (i.e., in the basis of the unperturbed WF ψ_1 and ψ_2) leads to the following relative intensities of the far and near satellite (in the case of observation in a direction perpendicular to $\mathbf{E}_0$):

$$\frac{S_\pm}{I_A}=\frac{E_0^2}{4(\Delta\pm\omega)^2}\,\frac{\sum\limits_{m,m',m''}|z_{12}|^2(|y_{20}|^2+|z_{20}|^2)}{\sum\limits_{m',m''}(|y_{20}|^2+|z_{20}|^2)}\,. \tag{2}$$

The summations over m, m', and m'' are needed because each of the levels 0, 1, and 2 can have several WF with different values of the magnetic quantum number.

Equation (2) is valid for relatively weak fields. Thus, e.g., in the case of low frequencies $\omega \ll \Delta$ it can be used under the condition

$$\max_{m,m''} \alpha(m, m'')\ll 1, \qquad \alpha(m, m'')=2E_0 z_{12}/\Delta. \tag{3}$$

To obtain results valid in stronger fields, we use the APT for the system with the two levels 1 and 2. It is known[16] that the instantaneous eigenvalues of the operator $H(t) = H_a + zE_0 \cos \omega t$ are

$$\omega_{1,2}(t)=[\omega_1^{(0)}+\omega_2^{(0)}\mp\Delta(1+\alpha^2\cos^2\omega t)^{1/2}]/2. \tag{4}$$

These eigenvalues correspond to the wave eigenfunctions (adiabatic basis)

$$\chi_1(t)=\psi_1\cos(\beta/2)-\psi_2\sin(\beta/2),$$

$$\chi_2(t)=\psi_1\sin(\beta/2)+\psi_2\cos(\beta/2),$$

$$\beta=\operatorname{arctg}(\alpha\cos\omega t). \tag{5}$$

We seek the solution of (2) in the form

$$\psi(t)=\sum_{j=1}^{2}C_j(t)\,\chi_j(t)\exp\Big[-i\int_0^t\omega_j(t')\,dt'\Big]. \tag{6}$$

Substitution of (6) in (1) yields

$$\dot{C}_1=-C_2(\dot{\beta}/2)\exp\left[-i\int_0^t\omega_{21}(t')\,dt'\right]$$

$$\dot{C}_2=C_1(\dot{\beta}/2)\exp\left[i\int_0^t\omega_{21}(t')\,dt'\right]; \tag{7}$$

$$\dot{\beta}/2=-\alpha\omega\sin\omega t/2(1+\alpha^2\cos^2\omega t). \tag{8}$$

We solve the system (7) by perturbation theory. To calculate the satellite intensities, the initial conditions $C_1(0) = 1$ and $C_2(0) = 0$ suffice. We then get from (7)

$$C_2(t)\approx\frac{1}{2}\int_0^t dt'\dot{\beta}(t')\exp\left[i\int_0^{t'}d\tau\omega_{21}(\tau)\right]. \tag{9}$$

To determine the integrals in (9) we expand $\beta(t)$ and $\omega_{21}(t)$ in Fourier series:

$$\dot{\beta}(t)=i(k\omega/4)\sum_{p=-\infty}^{+\infty}(a_{2p}-a_{2p+2})\times\exp[i(2p+1)\omega t],$$

$$\omega_{21}(t)=\bar{\Delta}+\sum_{q=1}^{+\infty}\varepsilon_{2q}\cos 2q\omega, \tag{10}$$

$$\bar{\Delta}\equiv(2/\pi)\Delta(1+\alpha^2)^{1/2}E(k),$$

where $k\equiv\alpha(1+\alpha^2)^{-1/2}$, $a_{2p}=2(-1)^p k^{-2|p|}[(1-k^2)^{1/2}-1]^{2|p|}$, $\varepsilon_2=(\frac{4}{3}\pi)\times\Delta(1+\alpha^2)^{1/2}[E(k)-2(1-k^2)D(k)]$; $E(k)$ and $D(k)$ are complete elliptic integrals. We consider hereafter only the case $\alpha\lesssim 1$, when it suffices to retain in $\beta(t)$ only the terms with $a_0=2$ and a_2. In the expansion of the exponential in (9) we confine ourselves to the expression

$$\exp\left[i\int_0^t d\tau\omega_{21}(\tau)\right]$$

$$\approx\left[J_0\left(\frac{\varepsilon_2}{2\omega}\right)+J_1\left(\frac{\varepsilon_2}{2\omega}\right)\exp(2i\omega t)-J_1\left(\frac{\varepsilon_2}{2\omega}\right)\exp(-2i\omega t)\right]\exp(it\bar{\Delta}). \tag{11}$$

The relative smallness of the discarded terms is determined numerically by the condition $\Delta/400\omega\ll 1$. Taking (10) and (11) into account we get from (9)

$$C_2(t)\approx(k\omega/8)\{[(2-a_2)J_0-2J_1]g(\bar{\Delta}+\omega)-[(2-a_2)J_0+2J_1]g(\bar{\Delta}-\omega)+(2J_1+a_2J_0)g(\bar{\Delta}+3\omega)+(2J_1-a_2J_0)g(\bar{\Delta}-3\omega),$$

$$g(u)\equiv[\exp(iut)-1]/u, \tag{12}$$

where the argument $\varepsilon_2/2\omega$ of the Bessel functions J_0 and J_1 is left out for brevity.

In the first nonvanishing order of the APT the WF of the two-sublevel system is thus of the form

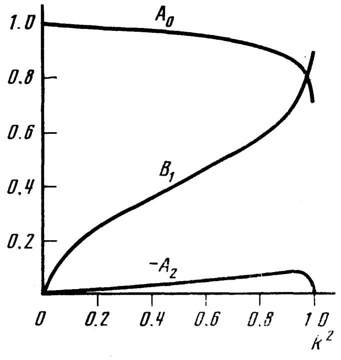

FIG. 1. The coefficients A_0, A_1, and B_1 of the Fourier expansions (15) of the adiabatic wave functions (5) vs the parameter $k^2\equiv\alpha^2/(1+\alpha^2)=4z_{12}^2E_0^2/(\Delta^2+4z_{12}^2E_0^2)$.

$$\psi(t)\approx\chi_1(t)\exp\left[-i\int_0^t dt'\omega_1(t')\right]+C_2(t)\chi_2(t)\exp\left[-i\int_0^t dt'\omega_2(t')\right]. \tag{13}$$

The spontaneous emission spectrum for the transition into the state 0 is calculated from the equation

$$I^{(e)}(\Delta\omega)=\lim_{T\to\infty}(2\pi T)^{-1}\left|\int_0^T dt\langle\psi(t)|\mathbf{re}|\psi_0\rangle\exp(-i\Delta\omega t)\right|^2, \tag{14}$$

where **e** is the unit vector of photon polarization.

To calculate the spectrum (14) we expand in Fourier series the functions $\sin(\beta/2)$ and $\cos(\beta/2)$ contained in $\chi_{1,2}(t)$:

$$\sin(\beta/2)=\sum_{p=0}^{\infty}B_{2p+1}\cos(2p+1)\omega t,$$

$$\cos(\beta/2)=\sum_{p=0}^{\infty}A_{2p}\cos 2p\omega t. \tag{15}$$

The dependences of the coefficients A_0, A_2, and B_1 on k^2 are shown in Fig. 1. We note that at $k^2\ll 1$ we have $A_0\approx 1-k^2/16$, $B_1\approx k/2+7k^3/64$, $A_2\approx -k^2/16$. We substitute the WF from (13) and (14), expressing the exponentials in (14) in a form similar to (11) and taking (4), (12), and (15) into account. We then obtain ultimately for the spectra $S_-^{(e)}$ and $S_+^{(e)}$ of the near and far satellites

$$S_{\mp}^{(e)}(\Delta\omega)=\sum_{m,m',m''}\sigma_{\mp}|\mathbf{r}_{20}\mathbf{e}|^2\delta[\Delta\omega-(\omega_{10}^{(0)}+\omega_{20}^{(0)}-\bar{\Delta})/2\mp\omega], \tag{16}$$

where $\bar{\Delta}(m,m'')$ is defined by (10), $\mathbf{r}_{20}(m'',m')\equiv\langle\psi_2|\mathbf{r}|\psi_0\rangle$, and for $\sigma_{\mp}(m,m'')$ we have

$$\sigma_-\approx\{(J_0-J_1)B_1/2+[(2-a_2)J_0(\varepsilon_2/2\omega)+2J_1(\varepsilon_2/2\omega)]\times J_0kA_0\omega/8(\bar{\Delta}-\omega)-(2A_0J_1+A_2J_0)J_0(\varepsilon_2/2\omega)k\omega/8(\bar{\Delta}+\omega)\}^2,$$

$$\sigma_+\approx\{(J_0+J_1)B_1/2-[(2-a_2)J_0(\varepsilon_2/2\omega)-2J_1(\varepsilon_2/2\omega)]\times J_0kA_0\omega/8(\bar{\Delta}+\omega)-(2A_0J_1-A_2J_0)J_0(\varepsilon_2/2\omega)k\omega/8(\bar{\Delta}-\omega)\}^2 \tag{17}$$

[the argument of the Bessel functions J_0 and J_1, whenever omitted from (17) for brevity, is $\varepsilon_2/4\omega$].

The spectrum of the allowed line is

$$I_A^{(e)}(\Delta\omega) \approx \sum_{m,m',m} (1-\sigma_- -\sigma_+)\,|\mathbf{r}_{20}\mathbf{e}|^2\delta[\Delta\omega-(\omega_{10}^{(0)}+\omega_{20}^{(0)}+\bar{\Delta})/2]. \quad (18)$$

We note that in (16) and (18) account is taken of the satellite-position shift

$$\delta(m, m'')=(\bar{\Delta}-\Delta)/2=[(2/\pi)(1+\alpha^2)^{1/2}E(k)-1]\Delta/2 \quad (19)$$

and of the equal but opposite shift of the allowed line.

The condition for the validity of the theory developed above is smallness of the coefficient $C_2(t)$ of the WF $\psi(t)$ in (13): $|C_2(t)|\ll 1$. In the case $\alpha \lesssim 1$ it suffices for this purpose, as seen from (12), to stipulate $\omega/\Delta \ll 1$.[2)]

2. Expressions (16)–(18) can be used to obtain the intensities of linearly polarized OEF in a plasma by measuring the ratio $S_{\mp}/I_A$. The region of their validity, in contrast to Refs. 1 and 14, is no longer limited to weak fields with $\alpha \ll 1$. By way of example, Fig. 2 shows (solid lines) the analytically calculated plots of S_+/I_A and S_-/I_A on $E_{\rm rms}=E_0/\sqrt{2}$ for the transitions $(4^1D, 4^1F)\to 2^1P$ in a helium atom, at two frequencies, $\omega=0.5$ cm^{-1} and $\omega=2$ cm^{-1} (the results are summed over the two polarizations). For comparison, the dashed line shows the analogous dependences from Ref. 11, where they were obtained numerically with a computer (we recall that we have used here the more accurate value $\Delta=5.43$ cm^{-1} from Ref. 13 instead of $\Delta=5.63$ cm^{-1} from Ref. 11). Of course, for another specified frequency ω used in a specific experiment it is also possible to carry out a relatively simple calculation with the aid of the analytic expressions (16)–(18).

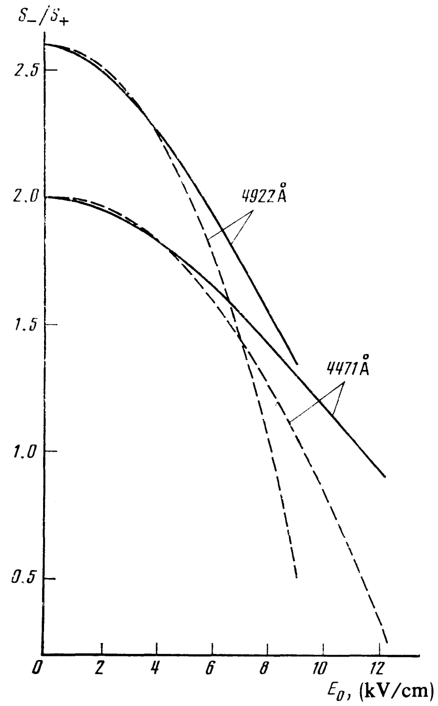

FIG. 3. Dependence of the intensity ratio S_-/S_+ of the near and far satellites on the amplitude E_0 of an oscillating field of frequency $\omega=1.28$ cm^{-1} for the lines He I 4922 Å and He I 4471 Å. Solid lines—results of adiabatic perturbation theory, dashed—results of Dirac perturbation theory (which is valid only at small E_0).

As noted in the Introduction, in a number of cases the volume v_E from which the satellites are emitted can be considerably smaller than the volume V from which the allowed spectral line is emitted. To determine the OEF intensity it is possible then to measure the satellite intensity ratio S_-/S_+. By way of example Fig. 3 shows (solid lines) plots of S_-/S_+ vs E_0 for the lines He I 4922 Å and He I 4471 Å, calculated from Eqs. (16) and (17) for the frequency $\omega=1.28$ cm^{-1} used in our experiment.

We point out that according to Eq. (2), obtained by the DPT with allowance for the terms $\propto E_0^2$, the ratio S_-/S_+ is constant. To obtain the dependence of S_-/S_+ on E_0 in the DPT the calculation must take into account at least terms $\propto E_0^4$. Such a calculation leads to the following satellite intensities:

$$\sigma_\pm \approx \frac{1}{(\Delta\pm\omega)^2}\left[\left(\frac{E_0 z_{12}}{2}\right)^2 \pm \left(\frac{E_0 z_{12}}{2}\right)^4 \frac{\Delta^3\mp 7\Delta^2\omega+3\Delta\omega^2\mp\omega^3}{\omega(\Delta^2-\omega^2)^2}\right]. \quad (20)$$

For illustration, the corresponding ratio $\varepsilon\sigma_-/\varepsilon\sigma_+$ is shown dashed in Fig. 3 (for the same frequency $\omega=1.28$ cm^{-1}). It can be seen that even when the terms $\propto E_0^4$ are taken into account, a DPT calculation is valid only for relatively weak fields.[3)]

3. The satellite polarization effect can be used to measure the degree of anisotropy of the OEF direction distribution or the angle between the vector $\mathbf{E}(t)=\mathbf{E}_0\cos\omega t$ and the

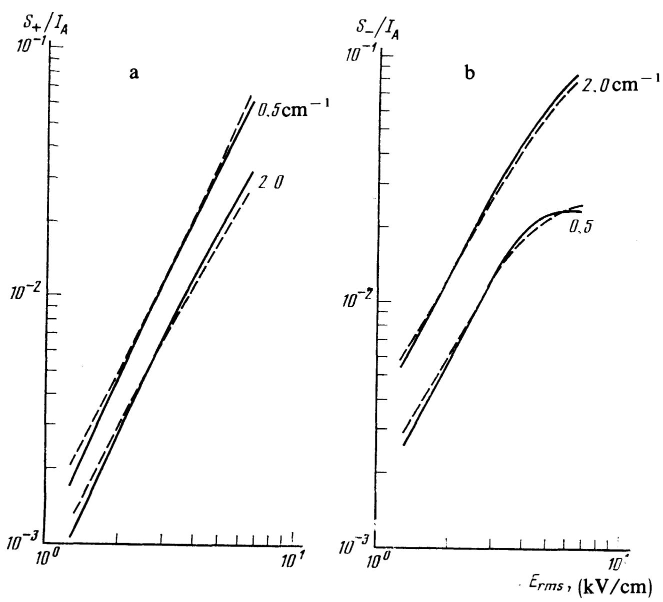

FIG. 2. Dependence of the ratio of the intensities of the far (a) or near (b) satellites to the intensity of the allowed line He I 4922 Å on the mean squared field $E_{\rm rms}=E_0/\sqrt{2}$ for two frequencies, $\omega=0.5$ cm^{-1} and $\omega=2$ cm^{-1}. Solid lines—analytic results of the present paper, dashed—results of computer calculations from Ref. 1.

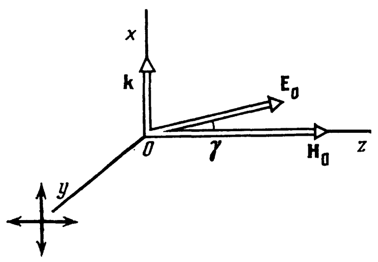

FIG. 4. Geometry of polarization observations. The z axis is chosen along the quasistationary magnetic field $\mathbf{H}_0$, and the x axis along the pump-wave vector $\mathbf{k}$. The observation is along the y axis. The amplitude E_0 of the oscillating field lies in the xz plane.

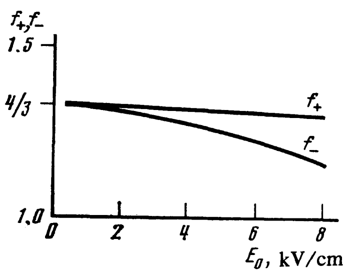

FIG. 5. Plots of the functions $f_+(E_0)$ and $f_-(E_0)$ from Eq. (22) that determines the intensity ratio of one and the same satellite at two mutually perpendicular positions of the polarizer.

polarizer transmission axis (which is usually determined by the symmetry axis of the experimental setup or by the directions of the polarization and of the wave vector of the external field). Assume that the observation is along the y axis (Fig. 4), the polarizer transmission axis is oriented in one case along the z axis and in the other along x, and the vector $\mathbf{E}$ is located in the xz plane and makes with the z axis an angle γ which is to be determined. From Eq. (16) for the satellite intensities $S^{(z)}_{\mp}$ (polarization along z) and $S^{(x)}_{\mp}$ (polarization along x) we then obtain

$$S^{(z)}_{\mp} = \sum_{m,m',m''} \sigma_{\mp}(|x_{20}|^2 \sin^2\gamma + |z_{20}|^2 \cos^2\gamma), \quad (21)$$

$$S^{(x)}_{\mp} = \sum_{m,m',m''} \sigma_{\mp}(|x_{20}|^2 \cos^2\gamma + |z_{20}|^2 \sin^2\gamma).$$

In practice it is convenient to measure the ratio of the intensities of one and the same satellite at two positions of the polarizer:

$$S^{(z)}_{\mp}/S^{(x)}_{\mp} = [1+f_{\mp}(E_0)\,\mathrm{ctg}^2\gamma]/[\mathrm{ctg}^2\gamma + f_{\mp}(E_0)], \quad (22)$$

$$f_{\mp}(E_0) = \Big(\sum_{m,m',m''} \sigma_{\mp}|z_{20}|^2\Big)\Big/\Big(\sum_{m,m',m''} \sigma_{\mp}|x_{20}|^2\Big).$$

We consider by way of example the transitions $(4^1F, 4^1D) \to 2^1P$. For weak fields we have $\sigma_{\mp} \approx (E_0 z_{12}/2(\Delta \mp \omega))^2$, and Eq. (22) yields $f_-(E_0) = f_+(E_0) = \frac{4}{3}$, which agrees with the result of Ref. 14. In other words, in weak fields the polarization-measurement results do not depend on the field amplitude. In strong fields the situation is different: The ratio $S^{(z)}_{\mp}/S^{(x)}_{\mp}$ depends not only on the angle γ but also on the field amplitude E_0. This is essentially a new factor compared with Ref. 14.

The functions $f_+(E_0)$ and $f_-(E_0)$ calculated from (22) and (17) are shown in Fig. 5. If the amplitude E_0 is known and $f_+(E_0)$ or $f_-(E_0)$ is found, we can determine from the experimentally measured ratio $S^{(z)}_{\mp}/S^{(x)}_{\mp}$ the angle γ with the aid of (22). We note, however, that in strong fields the values of f_- and f_+ approach unity (the degree of polarization of the satellites decreases), so that the angle γ is less accurately determined from (22).

§3. EXPERIMENTAL DETERMINATION OF OEF AMPLITUDES IN A PLASMA

1. The OEF amplitudes in a plasma were measured with the experimental setup illustrated in Fig. 6. What was investigated in this setup was the nonlinear interaction of electromagnetic radiation with a collisionless dense plasma. In earlier experiments[18,21] it was observed that when a certain threshold pump-wave electric field is exceeded nonlinear absorption of the electromagnetic radiation due to the development of parametric instability in the plasma, appears near the critical plasma density N_{cr} ($\varepsilon \approx 1 - N_e/N_{cr} \approx 0$).

The experimental setup and its operation were described earlier in Refs. 18–22; we point out here therefore only some essential details. The microwave source was a gyrotron generating 200-μsec pulses at a working wavelength $\lambda = 0.78$ cm. A linearly polarized wave was formed with the aid of corrector mirrors and was focused on the center of a vacuum chamber. The spatial distribution of the amplitude of the electric field at the focus of a teflon lens, in a plane perpendicular to the wave vector $\mathbf{k}$, was close to Gaussian:

$$E(y, z) = E_0 \exp[-(y^2+z^2)/a^2],$$

where $a \approx 1$ cm (the x axis is directed along $\mathbf{k}$). In this case the time-averaged power at the beam focus is $P = \varepsilon^{1/2} c a^2 E_0^2/16$, where ε is the dielectric constant. At $\varepsilon = 1$ the equation connecting E_0 with P is

$$E_0(\mathrm{V/cm}) \approx 22\ [P(\mathrm{W})]^{1/2}. \quad (23)$$

During the time of the microwave pump pulse, the plasma density increased smoothly and reached the critical (at the frequency $\omega = 1.28$ cm^{-1}) value $N_{cr} = 1.85 \times 10^{13}$ cm^{-3}. The optical radiation was introduced perpendicular to the plane of the vectors $\mathbf{k}$ and $\mathbf{E}_0$ and was analyzed by a DFS-12 monochromator with an instrumental-function half-width ≈ 0.2 Å. The radiation of the satellites entered the monochromator in this case from a strong-field region with linear dimension $L_E \sim a \sim 1$ cm, while the allowed-line radiation came from a region with linear dimension $L \gg L_E$. Because of the good reproducibility ($\approx 10\%$) of the parameters of the plasma and of the microwave, the contours of the spectral lines could be plotted "point by point." The spectral-line profiles were reduced for the instant of time t_1 when the plasma was transparent ($N < N_{cr}$, i.e., $\varepsilon > 0$) and for the

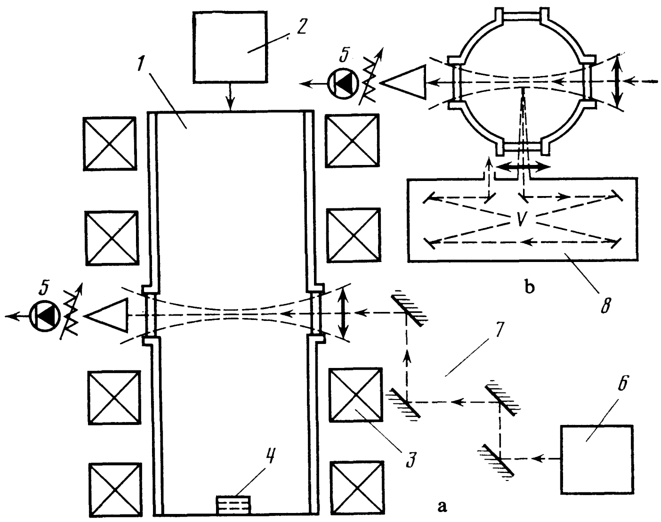

FIG. 6. Experimental setup: a) 1—vacuum chamber, 2—rf plasma source; 3—solenoid; 4—multigrid probe; 5—thermistor head; 6—gyrotron; 7—quasi-isotopic channel; 8—DFS-12 monochromator; b) top view.

instant t_2 when $N = N_{cr}$ (i.e., $\varepsilon = 0$) is reached and electromagnetic energy is nonlinearly absorbed.

2. Figure 7 shows a typical oscillogram of the emission of the satellite closest to the He I 4922 Å line. The steep increase of the satellite luminous emittance at the instant t_2 (while the emittance of the fundamental line remains practically constant) indicates an increase of the OEF amplitude in the plasma.

The optical measurements were made at pump microwave powers $P = 1.9$, 3.8, 7.5, 15, and 60 KW. By way of example, Figs. 8 and 9 shown emission spectra recorded respectively near the lines He I 4471 Å and He I 4922 Å at the instants t_1 and t_2 at a power $P = 60$ kW.

We note that near the 4471 Å line are observed not only two satellites, but also the OII 4469 Å line (owing to oxygen occlusion). We point out that at low powers, $P \ll 10$ kW, the satellite emission is weak and in practice one observes near the forbidden line only the OII 4469 Å line, which can be erroneously interpreted as a "solitary" satellite. It can be suggested in this connection that in those cases when other workers interpreted the spectrum observed near the He I 4472 Å as a solitary plasma satellite (see, e.g., Ref. 23), what was actually observed was the OII 4469 Å line.

3. The spectra near the 4471 Å and 4922 Å lines, recorded at the instant t_2 and at powers $P = 7.5$, 15, and 60 kW, were processed by measuring the ratio S_-/S_+. A subsequent comparison with the theoretical field dependences of S_-/S_+ (see Fig. 3) yielded the amplitude E_{0p} of the OEF in the region of plasma resonance ($\varepsilon = 0$). The amplitude E_{0r} of the field in a transparent plasma (at the instant t_1, when $\varepsilon > 0$) was determined as a rule from the known pump power P with the aid of Eq. (23) rather than from the experimental ratio S_-/S_+. The reason is that in a transparent plasma at powers $P \lesssim 15$ kW the far satellite is weak and its intensity was measured with a large error (the same situation is typical of the plasma-resonance region at powers $P \lesssim 4$ kW). At $P = 60$ kW, however, measurement of S_-/S_+ in a transparent plasma yielded $E_{0r} = 4.6 \pm 0.4$ and 6 ± 1 kW/cm for the lines 4922 and 4471 Å, respectively, which agrees with the value $E_{0r} = 5.4 \pm 0.5$ kW/cm obtained from Eq. (23).[4)] The results, including the field gain $K = E_{0p}/E_{0r}$, are listed in Table I.

We note that in the case of the He I 4471 Å line the emission of the OII 4469 Å impurity overestimates the intensity S_+ of the far satellite, and hence the amplitude E_0. Account was therefore taken in the calculation of K of the higher reliability of the data obtained for the He I 4922 Å line.

The OEF amplitudes were estimated also from the measured ratio S_-/I_A in order to illustrate the substantial effect of the spatial form factor, as well as to estimate roughly the field at low powers $P < 4$ kW, at which the ratio S_-/S_+ cannot be measured reliably. The measurement results averaged over two lines (4922 Å and 4471 Å) are shown in Fig. 10.

The straight line in Fig. 10 corresponds approximately to the case of a transparent plasma. It was drawn through the vertical error bar of E_{0r} determined from the ratio S_-/I_A measured at the instant t_1 for $P = 60$ kW. It follows from the slope of this line that the real value of the amplitude $E_0^{\rm real}$ is approximately 2.8 times larger than $E_0^{\rm exp}$ determined by measuring S_-/I_A. We can then estimate roughly the spatial form factor at $L/L_E \sim (2.8)^2 \approx 8$. The obtained value $L \sim 8L_E \sim 8$ cm agrees with the half-width of the spatial distribution of the plasma density over the chamber diameter.

The error bars above the line in Fig. 10 correspond to

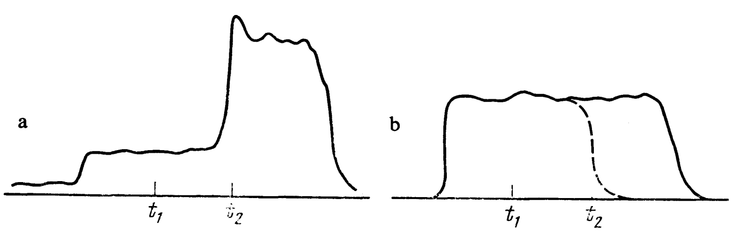

FIG. 7. a) Typical oscillogram of the emission of the satellite closest to the He I 4922 Å line. b) Incident (solid curve) and transmitted (dashed) microwave signal. The instant t_2 corresponds to $\varepsilon = 0$ ($N_e = N_{cr}$).

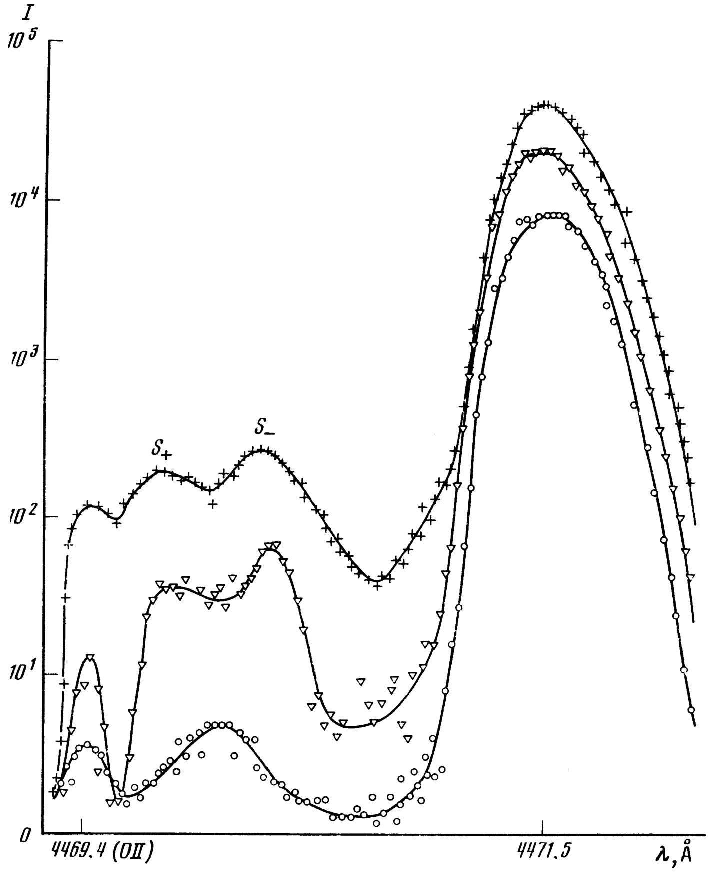

FIG. 8. Spectrum near the He I 4471 Å line at a pump microwave power $P = 60$ kW for three plasma regions: crosses—region of plasma resonance ($N_e = N_{cr}$, $\varepsilon = 0$); triangles—plasma-transparency region ($N_e < N_{cr}$, $\varepsilon > 0$); points—region without microwave field. The OII 4469 Å line can also be seen.

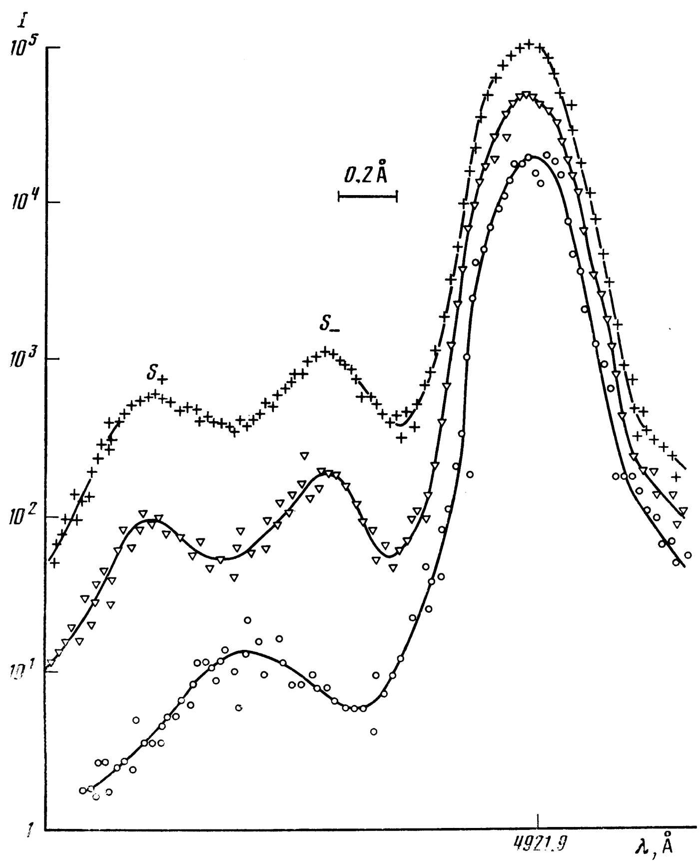

FIG. 9. The same as Fig. 8, but near the He I 4922 Å line.

TABLE I.

P kW	E_{0r} kV/cm	E_{0p} kV/cm		$K=E_{0p}/E_{0r}$
		4922 Å	4471 Å	
7.5	1.9±0.2	6.4±0.4	$6.5^{+0.5}_{-1}$	3.4±0.6
15.0	2.7±0.3	6.1±0.4	$7.0^{+0.5}_{-1}$	2.4±0.5
60.0	5.4±0.5	6.2±0.4	$8.0^{+0.5}_{-1}$	1.3±0.3

plasma resonance ($\varepsilon = 0$) at powers $P = 1.9$, 3.8, 7.5, 15, and 60 kW. For a rough estimate of the real amplitude E_0^{real}, each value of E_0^{exp} should also be multiplied by 2.8. At $P = 7.5$, 15, and 60 kW, the estimates of E_0 obtained in this manner can be compared with the more rigorous results in the table, and the agreement between them verified.

4. The results offer evidence that the electric-field gain in the plasma resonance region ($\varepsilon = 0$) has a maximum at $E_{0r} \sim 2$ kW/cm and decreases with increasing field in the pump wave. The amplitude of the electric field E_{0p} does not exceed $E_{\max} \sim 7$ kW/cm. It is of interest to determine not only the amplitude but also the predominant direction of the electric field at $\varepsilon = 0$. This is made possible by the polarization technique whose results are reported below.

§4. POLARIZATION TECHNIQUE

1. To determine the predominant direction of the electric field we used a polarizer placed ahead of the entrance into the DFS-12 monochromator. The radiation intensity of the near satellite of the He I 4922 Å line was recorded at two positions of the polarizer transmission axis, along the electric field in the pump wave (this coincides with the direction of the quasistationary magnetic field in the plasma, or the z axis of Fig. 4) ($S_-^{(z)}$), and perpendicular to this direction (i.e., along the wave vector **k** parallel to the x axis in Fig. 4) ($S_-^{(x)}$). The statistical reduction of each measurement of the polarized-radiation intensity $S_-^{(z)}$ or $S_-^{(x)}$ was carried out over 30 points. The results of the statistical reduction (including the standard error) are the following:

P, kW	1.3	4	13	40
$S_-^{(z)}/S_-^{(x)}$	1.008±0.026	0.956±0.014	0.942±0.017	0.994±0.014

Using these data and Eq. (22) we determined the value of $\cot^2\gamma \equiv E_z^2/E_x^2$. This procedure included the determination of the amplitude E_{0p} (by the procedure described in §§2 and 3), determination of $f_-(E_{0p})$ (see Fig. 5), and only then followed by a direct calculation of $\cot^2\gamma$ from Eq. (22). The obtained dependence of E_z^2/E_x^2 on the pump field E_0 is shown in Fig. 11. It can be seen that the enhancement of the electric field in the plasma-resonance region is due to a considerable degree to the appearance of the E_k component (parallel to **k**), which was practically nonexistent in the pump wave. This effect is maximal at E_{0r} 2.5 kW/cm. With increasing pump field, the longitudinal and transverse components of the field E_{0p} become of the same order ($E_z \approx E_x$).

2. For further illustration, we determined in experiment the predominant direction the pump field in a transparent plasma at $P = 40$ kW. Statistical reduction of the experiment yielded $S_-^{(z)}/S_-^{(x)} = 1.183 \pm 0.026$. The measurements were made at a plasma density $N \approx 0.5 N_{0r}$, corresponding to $\varepsilon \approx 0.5$. In this case we have in lieu of (23) E_0 (V/cm) $\approx 26 [P(\text{W})]^{1/2}$. A power $P = 40$ kW corresponds to an amplitude $E_0 \approx 5.2$ kW/cm, at which $f_-(E_0) \approx 1.24$. Using (22), we obtain $E_z^2/E_x^2 = 8^{+8}_{-3}$. The relatively large spread is due to the fact that according to (22) $\cot^2\gamma \propto [f_-(E_{0r}) - S_-^{(z)}/S_-^{(x)}]^{-1}$, and the values of f_- and

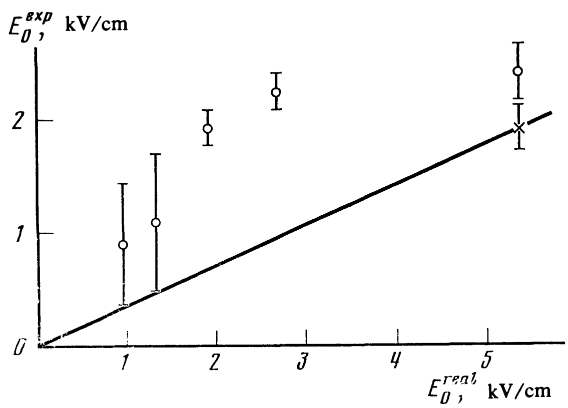

FIG. 10. Connection between the field E_0^{exp} determined experimentally by measuring the ratio S_-/I_A for the lines 4922 Å and 4471 Å with the real field E_0^{real}; this connection results from the presence of the spatial form factor. (The values of E_0^{exp} were obtained by averaging the results obtained for each of the lines 4922 Å and 4471 Å.)

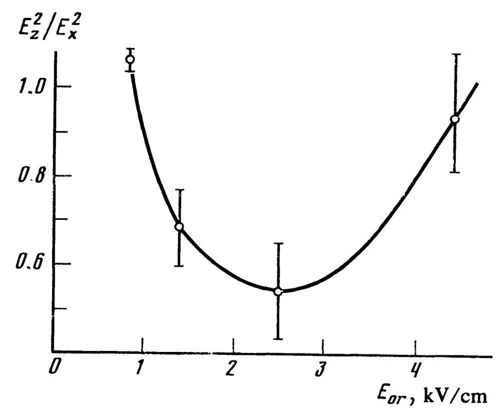

FIG. 11. Dependence of the ratio E_x^2/E_z^2 in the region of the plasma resonance on the pump field E_0, as obtained in experiment with the aid of polarization analysis.

$S_-^{(z)}/S_-^{(x)}$ are close in this case.

It was known beforehand that the E_z component predominates in the focused microwave beam, and that in the $y = 0$ plane

$$E_z = E_0 \exp(-z^2/a^2) \exp(i\omega t - ik_0\varepsilon^{1/2}x). \quad (24)$$

Such a beam, however, should have also an E_x component. In fact, substituting (24) in the condition div $\mathbf{E} = 0$ we obtain

$$E_x = (2zE_0/k_0\varepsilon^{1/2}a^2) \exp(-z^2/a^2) \exp(i\omega t - ik_0\varepsilon^{1/2}x + i\pi/2). \quad (25)$$

Consequently $|E_x^2/E_z^2| = (2z/k_0\varepsilon^{1/2}a^2)^2$. Calculating the spatial mean value, we get $\langle |E_x^2/E_z^2| \rangle \approx \frac{1}{16}$, which agrees with the result of polarization measurements within the standard error.

We note in conclusion the polarization-analysis results in the present paper, with account taken of the function $f_-(E_0)$ in (22), differ substantially from the results that would be obtained from the corresponding formula of Ref. 14 (i.e., replacing f_- by 4/3). In particular, the minimum of the curve of Fig. 11 (which demonstrates the effect of field enhancement along **k**) would be reached at $E_{0r} = 1.4$ kV/cm in lieu of $E_{0r} = 2.5$ kV/cm, and the result of the control experiment for a microwave beam in a transparent beam would be of the form $E_z^2/E_x^2 = 4 \pm 1$, strikingly different from the real value $\langle |E_x^2/E_z^2| \rangle \approx \frac{1}{16}$.

§5. DISCUSSION OF RESULTS

1. We have developed an adiabatic theory of forbidden-line satellites for the case of low frequencies $\omega \ll \Delta$. This theory turns out to be valid not only in weak but also in strong fields, for which the heretofore existing solutions (obtained with the aid of the DPT) do not hold.

Starting from the indicated analytic results, a new principle was proposed for measuring the amplitude E_0 of EOF in a plasma. The principle is based on comparing the experimental ratio of the satellite intensities with the theoretical dependence of S_-/S_+ on E_0. This principle permits, in essence, local measurements of the amplitude E_0 in the strong-field region (which can be considerably smaller than the effective volume of the radiating plasma), without resorting to complicated experimental techniques such as resonant fluorescence.

Finally, with the aid of the adiabatic theory of the satellites we have succeeded in extending into the strong field region the technique proposed in Ref. 14 for polarization analysis of OEF. It should be noted that the theory developed is applicable to OEF diagnostics using the spectra of multiply charged helium-like ions, for which the condition $\omega \ll \Delta$ usually holds.

2. The diagnostic procedures indicated above were successfully tested in experiments on the interaction of a powerful microwave with an inhomogeneous plasma. The results of the reduction of the spectra of several helium lines, observed in both unpolarized and polarized light, permit the following conclusions to be drawn.

Amplification of the OEF, $E_{0p} > E_{0r}$, takes place when the threshold field $E_{0r}^{\min} \sim 0.5$ kV/cm is exceeded in the pump wave near the critical-density surface ($N \approx N_{cr}$, $\varepsilon = 0$). The function $E_{0p}(E_{0r})$ is nonlinear. The amplitude gain $K = E_{0p}/E_0r$ has a maximum at $E_{0r} \sim 2$ kV/cm. When the pump field is increased the gain "saturates" and the electric-field amplitude E_{0p} does not exceed $E_{\max} \sim 7$ kV/cm. For a plasma with parameters $N \sim 2 \times 10^{13}$ cm^{-3} and $T_e \sim 10$ eV ($T_i \approx 1$ eV) this means that the energy density of the intraplasma OEF is $W \lesssim 10^{-1} NT_e$. These conclusions agree with results of spectroscopic investigations made with the same apparatus and based on an analysis of the profiles of the hydrogen line H_β (Ref. 22).

The polarization measurements have shown that in the region of plasma resonance there is preferred amplification of the longitudinal component of the electric field (parallel to the vector **k** of the pump wave). This effect is a maximum at a pump amplitude $E_{0r} \approx 2.5$ kV/cm, at which the ratio of the energy densities of the longitudinal field components for $\varepsilon = 0$ and for $\varepsilon > 0$ is $\sim 10^2$.

The earlier experiments with this setup[18-20] revealed a number of other nonlinear effects: generation of fast electrons, evolution of ion-sound oscillations, and superthermal electromagnetic radiation near the plasma frequency. All these facts allow us to conclude that action of a powerful electromagnetic wave on a collisionless plasma produces in the latter parametric instability and excites plasma turbulence, including intense Langmuir oscillations whose energy density is much higher than in the pump wave.

[1)]We note in this connection a recent paper[15] in which it is proposed to use laser excitation at the wavelength of the allowed He I 3965 Å line, followed by observation near the forbidden He I 4911 Å line.

[2)]A more general condition for the applicability of the theory (valid also at $\alpha \gg 1$) is $\alpha\omega/2\Delta \ll 1$. We note that to find the WF $\psi(t)$ and the spectrum $I(\Delta\omega)$ at $\alpha \gg 1$ it is necessary to include a large number of terms in the expansions (10), (11), and (15).

[3)]We note that in the presence of a spatial form factor we can use for the quasi-local measurements not only the ratio S_-/S_+ but also the shift $\delta(m,m'')$ of the satellite components [see Eq. (19)]. A similar measurement principle is proposed in Ref. 17, where an approximation based on a computer calculation of the spectrum is given for the dependence of the shift on $E_{\rm rms}$ (for the He I 4922 Å line).

[4)]The error of (23) is due to two factors. First, it was obtained for $\varepsilon = 1$, whereas $\varepsilon < 1$ in a transparent plasma. Second, at a given P it would be necessary, for comparison with experiment, to use an equation such as (23) to determine not E_0, but a certain effective amplitude $E_0^{\rm eff} < E_0$. Thus, for example, averaging of the values of S_- and S_+ over a Gaussian distribution of the amplitudes in space yields $E_0^{\rm eff} \approx 0.8 E_0$. Fortunately the foregoing two circumstances cancel each other to a considerable degree.

[1]M. Baranger and B. Mozer, Phys. Rev. **123**, 25 (1961).
[2]G. Bekefi and C. Deutsch, Comments Plasma Phys. **2**, 89 (1976).
[3]Ya. F. Volkov, V. G. Dyatlov, and N. I. Mitina, Preprint No. 78-54, Khar'kov Physicotech. Inst., 1978.
[4]E. I. Kuznetsov and D. A. Shcheglov, Metody diagnostiki vysokotemperaturnoĭ plazmy (Methods of High-Temperature-Plasma Diagnostics), Atomizdat, 1980.
[5]Y. S. Al-Shiraida, A. Hirose, and H. M. Skarsgard, Canad. J. Phys. **57**, 845 (1979).
[6]J. Hildebrandt and H.-J. Kunze, Phys. Rev. Lett. **45**, 183 (1980).
[7]D. Prosnitz, D. W. Wildman, and E. V. George, Phys. Rev. A **13**, 891 (1976).
[8]S. H. Kim and H. Y. Chung, J. Appl. Phys. **49**, 5081 (1978).
[9]V. P. Gavrilenko and E. A. Oks, Internat. Conf. on Plasma Phys., Goteborg, June 1982, 14P-I-10, p. 336.

[10]H.-J. Kunze, H. R. Griem, A. W. da Silva, G. C. Goldenbaum, and I. Spalding, J. Phys. Fluids **12**, 2669 (1969).
[11]W. W. Hicks, R. A. Hess, and W. S. Cooper, Phys. Rev. A **5**, 490 (1972).
[12]S. H. Autler and C. H. Townes, Phys. Rev. **100**, 703 (1955).
[13]W. C. Martin, J. Phys. Chem. Ref. Data **23**, 257 (1973).
[14]W. S. Cooper and H. Ringler, Phys. Rev. **179**, 226 (1969).
[15]T. Oda and K. Kawasaki, Jpn. J. Appl. Phys. **20**, L761 (1981).
[16]A. S. Davydov, Quantum Mechanics, Pergamon, 1965, §49.
[17]W. S. Cooper and H. Ringler, Phys. Rev. **179**, 226 (1969).
[18]V. G. Eremin, A. V. Kostrov, A. D. Stepanushkin, and G. M. Fraiman, Fiz. Plazmy **2**, 414 (1976) [Sov. J. Plasma Phys. **2**, 226 (1976)].
[19]V. G. Eremin, A. V. Kostrov, N. V. Lukin, and A. D. Stepanushkin, Izv. Vyssh. Ucheb. Zaved. Radiofizika **20**, 1489 (1977).
[20]V. G. Eremin, A. V. Kostrov, and A. D. Stepanushkin, Fiz. Plazmy **5**, 1176 (1979) [Sov. J. Plasma Phys. **5**, 661 (1979)].
[21]M. P. Brizhinev, S. V. Egorov, B. G. Eremin, A. V. Kostrov, and A. D. Stepanushkin, J. de Phys. **40**, C7-867 (1979).
[22]M. P. Brizhinev, S. V. Egorov, B. G. Eremin, A. V. Kostrov, E. A. Oks, and Yu. M. Shagiev, 15th Internat. Conf. on Phenomena in Ionized Gases, Minsk, July 1981, P-1714, p. 971.
[23]G. V. Zelenin, A. A. Kutsyn, M. E. Maznichenko, O. S. Pavlichenko, and V. A. Suprunenko, Zh. Eksp. Teor. Fiz. **58**, 1879 (1970) [Sov. Phys. JETP **31**, 1009 (1970)].

Translated by J. G. Adashko